Supplementary material

Rapid and High-Concentration Exfoliation of Montmorillonite into High-Quality and Mono-Layered Nanosheets

Zhengmao Ding[1,2], Jie Li[1], Bowen Zhang[1,2], Yunjun Luo[1,2]*

[1]School of Materials Science and Engineering, Beijing Institute of Technology, Beijing, 100081, China.

[2]Key Laboratory of High Energy Density Materials, Ministry of Education, Beijing Institute of Technology, Beijing 100081, China.

Correspondence and requests for materials should be addressed to Y.L. (email: yjluo@bit.edu.cn)

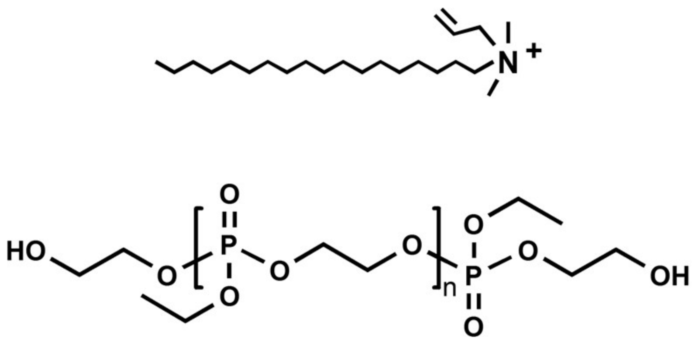

ODAAC

Exolit OP 550

Figure S1. Chemical structure of ODAAC and Exolit OP 550.

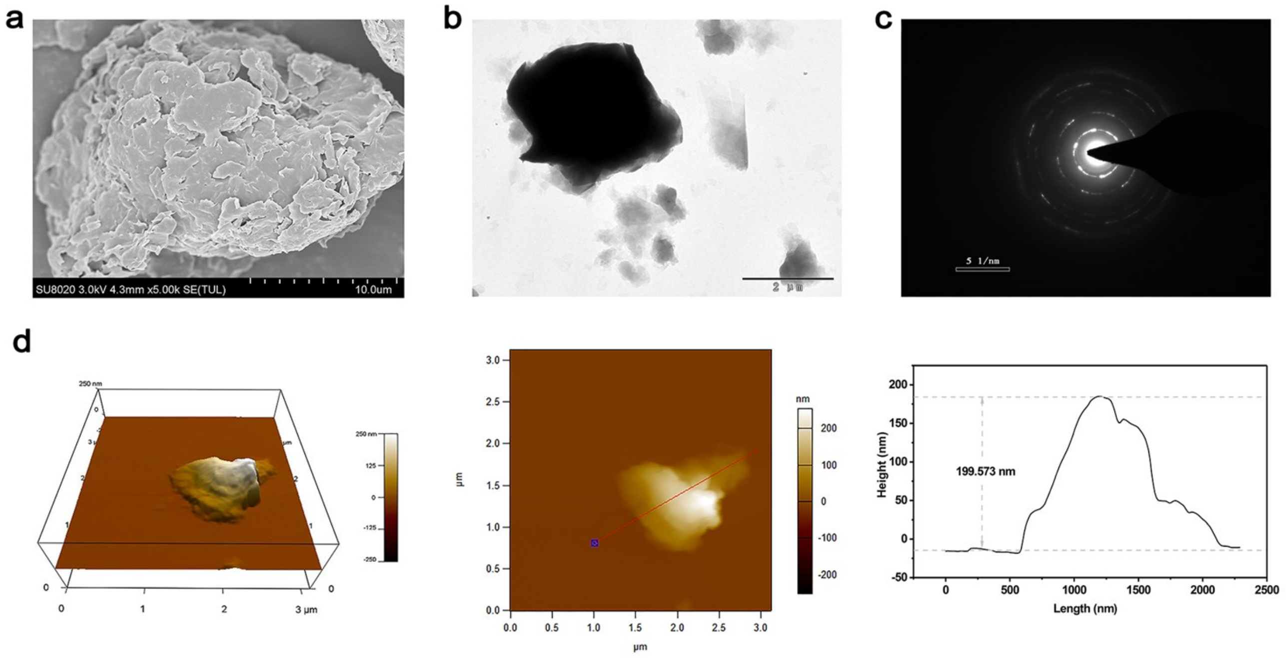

Figure S2. Characterization of OMTM. a) SEM image of OMTM. *Scale bar*, 10.0 μm. The appearance of the OMMT material used in this paper appears as millimeter-scale agglomerated particles, which are formed by agglomeration of many micrometer scale layered primary particles. **b)** Typical TEM image of OMTM. *Scale bar*, 2 μm. It is visually opaque black, indicating that the OMTM agglomerated particle is thick. **c)** SAED pattern of OMTM. *Scale bar*, 5 1/nm. The crystal structure of OMTM belongs to monoclinic crystal system. The diffraction ring indicates that the OMTM is multi-layered, and the arrangement of layers is irregular. **d)** AFM image, the corresponding topological image, and the height profile of OMTM. *z scale*, -250.0 to 250.0 nm. The thickness is measured to be ~199.573 nm.

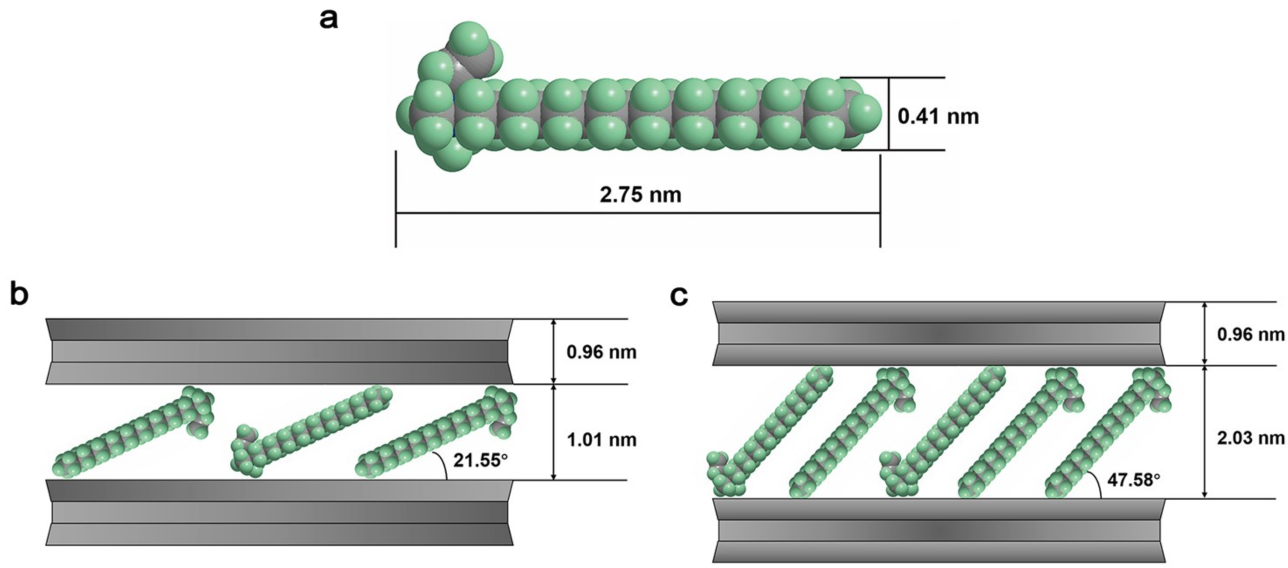

Figure S3. Configuration of ODAAC in OMTM interlayer. a) Space-filling model of ODAAC molecular chain. **b, c)** Assembly manner of ODAAC in OMTM interlayer.

In the ideal space-filling model of ODAAC, the length of the molecular chain is 2.75 nm.[1] The tilting angle θ of the ODAAC chains in the interlayer space could be calculated by Eq. (3)[2]:

$$\sin\theta = \frac{d - d_0}{L} \tag{3}$$

where d_0 was the thickness of MTM nanosheet, d was the interlayer distances of OMTM, and L was the length of the ODAAC chain. Since the interlayer distances of OMTM were 2.80 nm and 2.09 nm, and the thickness of MTM nanosheet was 0.96 nm, it could be speculated that the ODAAC in the interlayer space adopted a paraffin-type monolayer configuration and the tilting angle θ with respect to the layer plane were calculated as 21.55° and 47.58°, respectively.

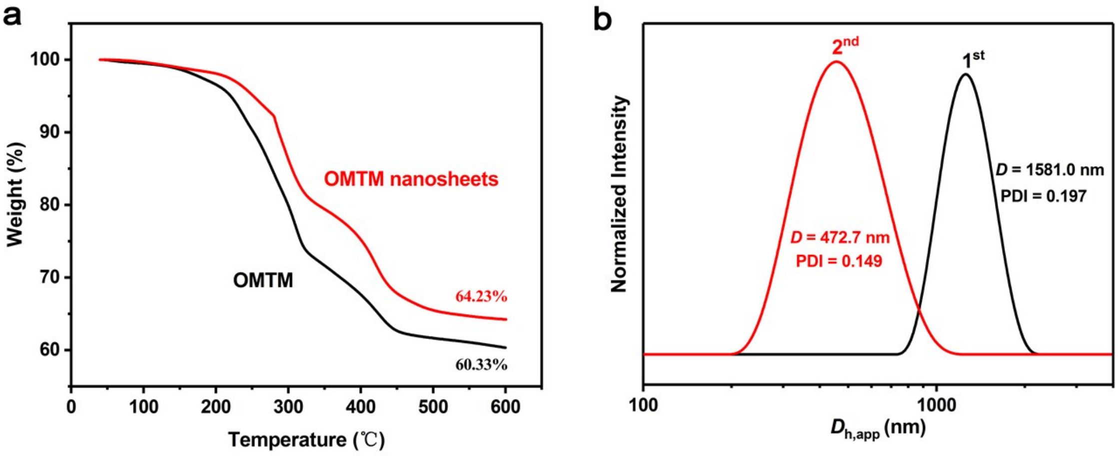

Figure S4. TGA and DLS characterization of OMTM nanosheets. a) TGA curves of OMTM and OMTM nanosheets prepared by washing with ethanol for twice to remove redundant polymer. The OMTM nanosheets were obtained from 20 wt.%OMTM/Exolit OP 550 nanocomposites prepared by 3 min mixing at 25 °C and 12 h ripening at 60 °C, and were dehydrated for 8 h in vacuum at 80 °C before use. It shows that most of the organics in the nanocomposites are removed after twice ethanol washes, which is even less than the organic content in the initial OMTM. **b)** Particle size distributions of the OMTM nanosheets after washed once and twice with ethanol. It shows that the particle diameter of OMTM/Exolit OP 550 nanocomposites decreased from 1581.0 nm (after the first washing, 1st) to 472.7 nm (after the second washing, 2nd).

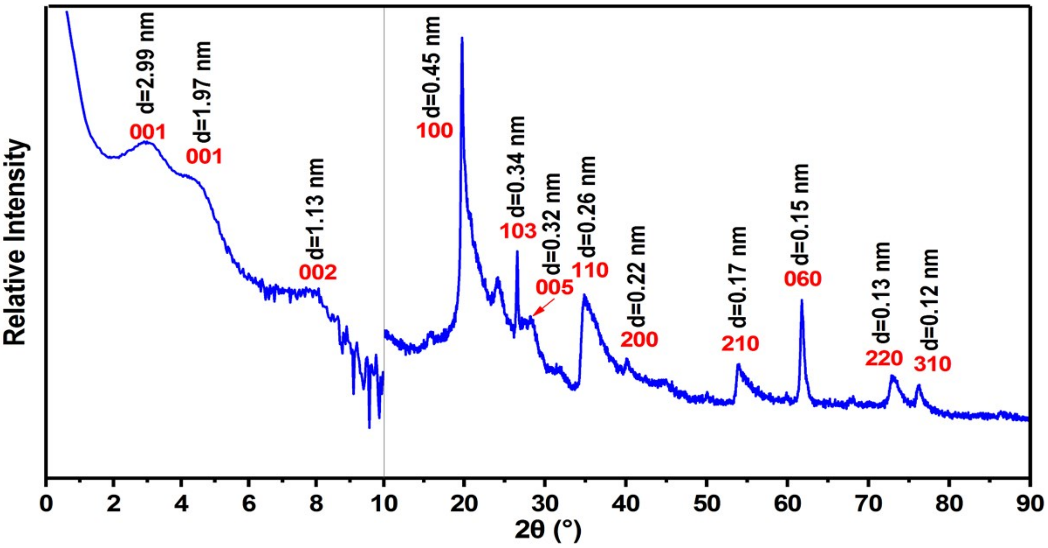

Figure S5. XRD pattern of OMTM.

It shows that the positions (interlayer distances and crystalline planes) of the main diffraction peaks of OMTM are 2.96° (2.99 nm and 001), 4.49° (1.97 nm and 001), 7.80° (1.13 nm and 002), 19.74° (0.45 nm and 100), 26.59° (0.34 nm and 103), 28.26° (0.32 nm and 005), 34.86° (0.26 nm and 110), 40.14° (0.22 nm and 200), 53.92° (0.17 nm and 210), 61.77° (0.15 nm and 060), 72.94° (0.13 nm and 220), and 76.24° (0.12 nm and 310), respectively. The crystal structure of MTM belongs to monoclinic crystal system. The main XRD diffraction peaks are consistent with those of No. 00-013-0135 in ICDD-PDF card.

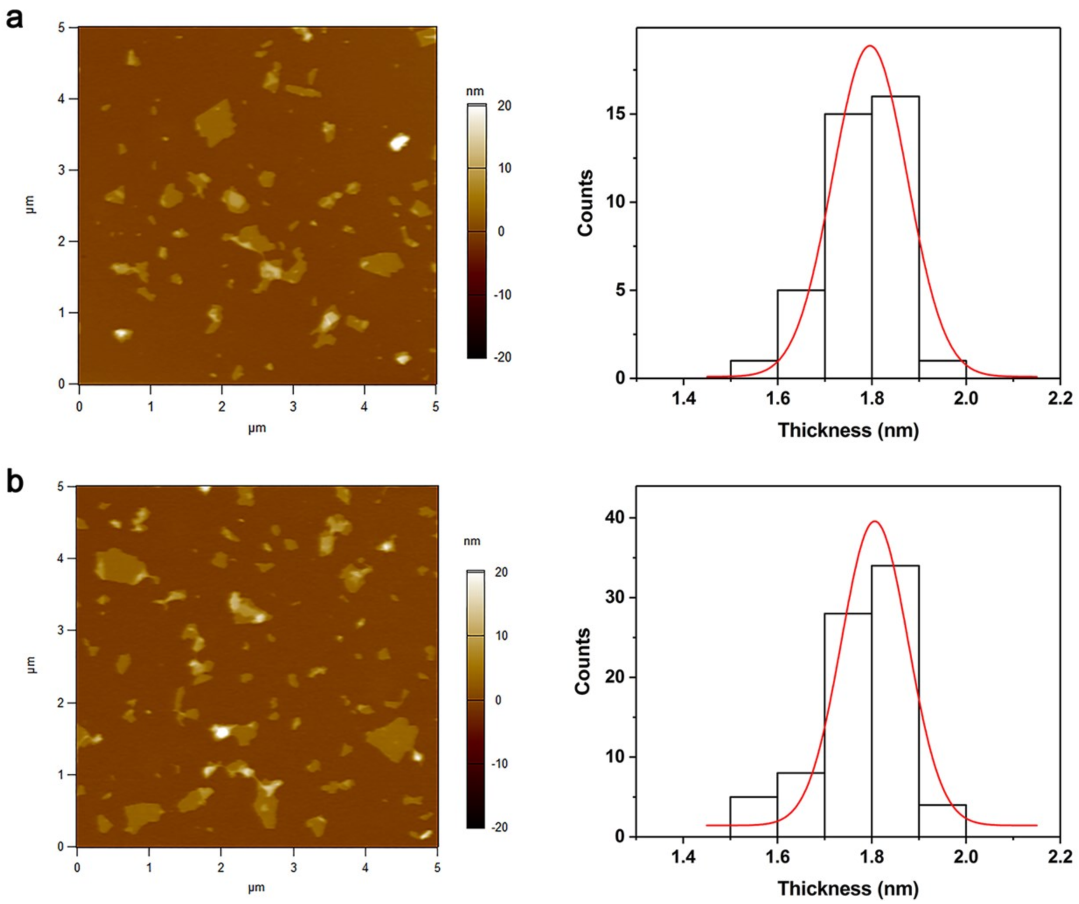

Figure S6. Histogram of the OMTM nanosheets thicknesses. a) OMTM nanosheets from 20 wt.% OMTM/Exolit OP 550 nanocomposites. **b)** OMTM nanosheets from 100 wt.% OMTM/Exolit OP 550/ethanol nanocomposites.

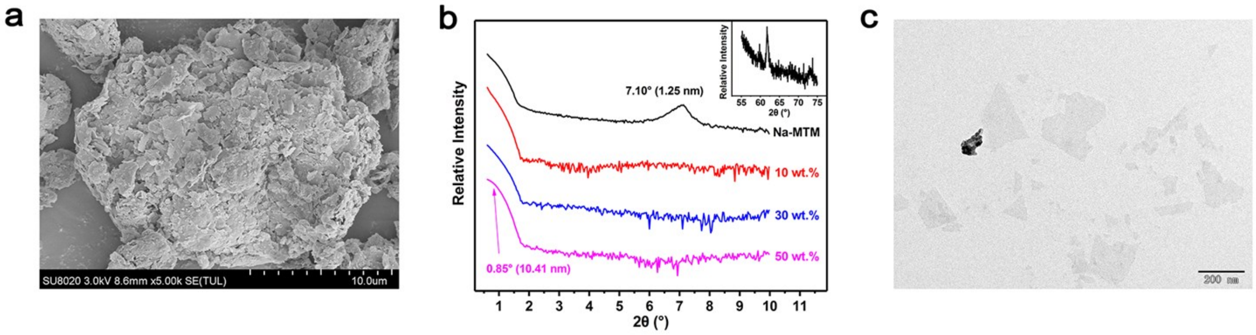

Figure S7. Characterization of Na-MTM. a) SEM image of Na-MTM. *Scale bar*, 10.0 μm. The Na-MMT appears as millimeter-scale agglomerated particles, which are formed by agglomeration of many micrometer scale layered primary particles. **b)** Small-XRD patterns of Na-MTM and Na-MTM/Exolit OP 550 nanocomposite after mixing for 3 min at 25 °C and ripening for 12 h at 60 °C. It shows that the diffraction peak of 30 wt.% Na-MTM/Exolit OP 550 nanocomposite at ~7.10° disappears, while a new diffraction peak of 50 wt.% Na-MTM/Exolit OP 550 nanocomposite at ~0.85° appears, confirming that the maximum exfoliation amount of Na-MTM in Exolit OP 550 could reached 30 wt.%. Inset shows the intrinsic diffraction peak of OMTM from 060 crystalline plane, confirming that test area contains sufficient concentration of OMTM to be tested. **c)** TEM image of the as-obtained Na-MTM nanosheets of 30 wt.% Na-MTM/Exolit OP 550 nanocomposites prepared by 3 min mixing at 25 °C and 12 h ripening at 60 °C. *Scale bars*, 200 nm. It shows that the nanosheets possess complete and uniform contrast, indicating no obvious defects on these nanosheets.

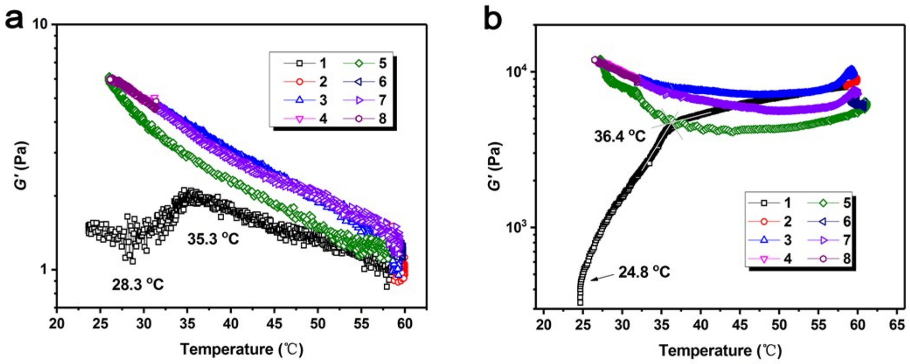

Figure S8. Non-isothermal ripening characterization. The *G´* of **a)** 10 wt.% and **b)** 30 wt.% OMTM/Exolit OP 550 nanocomposites with two heating and cooling cycles scans, respectively. Processes 1 and 5 are heating scans, processes 3 and 7 are cooling scans, and other processes are heat preservation scans. The nanocomposites were prepared by mixing OMTM and Exolit OP 550 at 25 °C for 3 min.

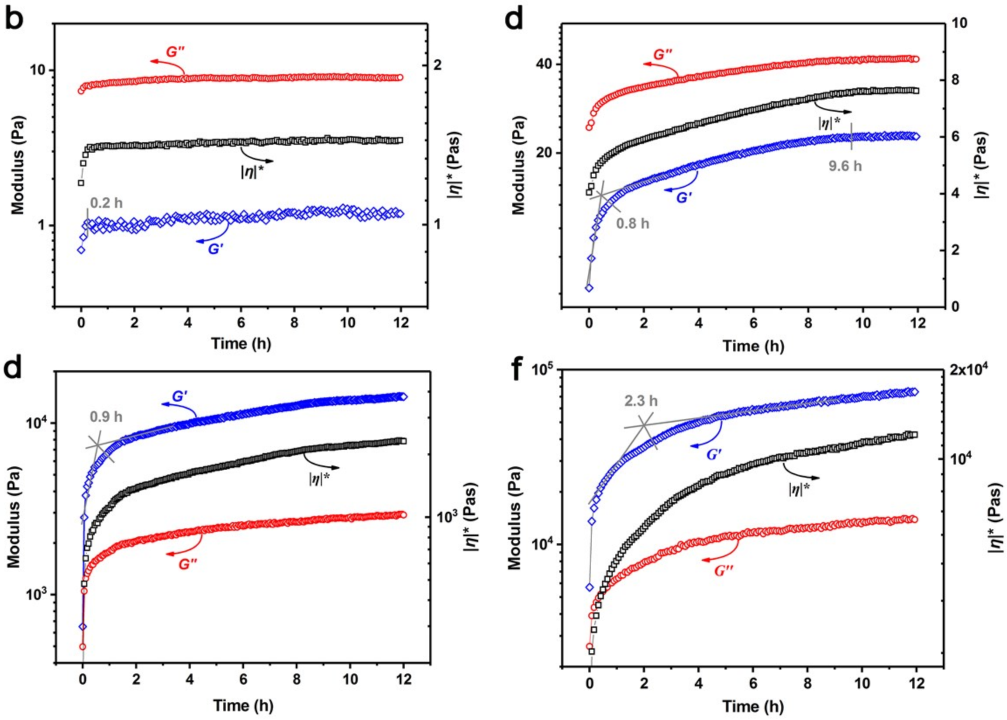

Figure S9. Isothermal ripening characterization. The *G´*, loss modulus (*G´´*), and complex viscosity (|*η*|*) of OMTM/Exolit OP 550 nanocomposites at 60 °C with different OMTM contents: **a)** 10 wt.%, **b)** 20 wt.%, **c)** 30 wt.%, **d)** 40 wt.%. The nanocomposites were prepared by mixing OMTM and Exolit OP 550 for 3 min at 25 °C.

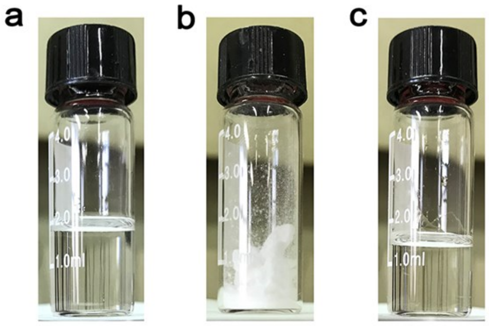

Figure S10 Turbidity characterization. a) Exolit OP 550. **b)** ODAAC. **c)** 5wt.% ODAAC/Exolit OP 550.

To check the affinity between the ODAAC and Exolit OP 550, we prepared mixtures by simple mixing them at 60 °C and then cooled to room temperature. It is interesting to note that ODAAC was readily dissolved in Exolit OP 550 as the mixture of ODAAC/Exolit OP 550 was clear. This may be interpreted by the presence of the –OH and –O- in Exolit OP 550 and its interaction to the polar head of the ODAAC.

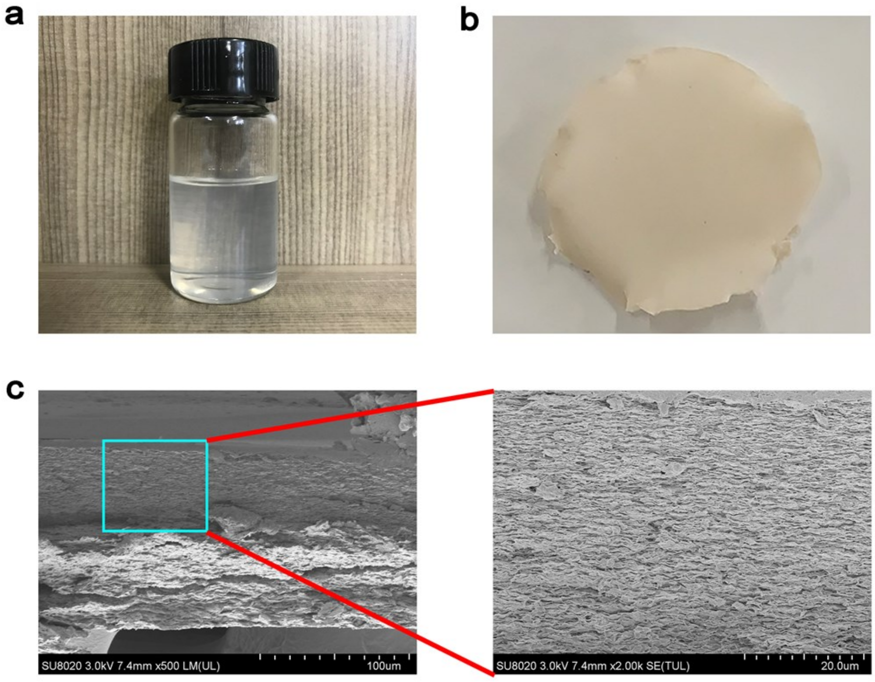

Figure S11. Structural characterization of the inorganic layered composite thin films. a) Photograph of the OMTM nanosheets dispersed in ethanol. **b)** Photograph of the nacre-like 80 wt.% MTM-PVA film prepared by vacuum filtration according to Ding *et al.*[3] **c)** Cross-sectional SEM images of the MTM-PVA film with different magnification. *Scale bars*, 100 µm and 10 µm.

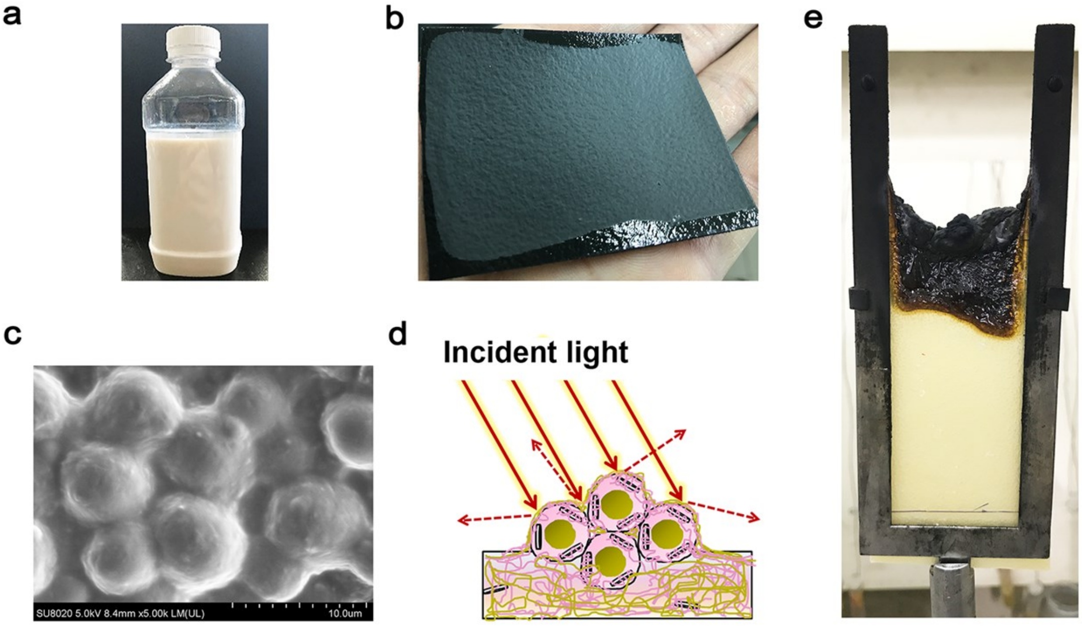

Figure S12. Multi-functionality organic hybrid nanocomposites. a) The waterborne polyurethane (WPU) emulsion based on OMTM and Exolit OP 550 prepared by in-situ polymerization. **b)** Photograph of the WPU nanocoating on polyvinyl chloride leathers by a scraping method. It exhibits superior low gloss performance, which is highly desirable properties for surface science. **c)** SEM image of the nanocoating surface. Scale bar, 10 μm. **d)** Schematic illustration of mechanism for the low gloss performance. **e)** Photographs of burning residues for the OMTM/WPU nanofilm collected after continuous combustion for 180 s under 23 vol.% oxygen concentration. The film exhibits favorable fire retardancy.

Table S1. Comparison of MTM production rates in our method with those of other previous works.

Sample	Method	Reagent	Key Conditions	$C_{e\text{-}MTM}$	Ref.
Na-MTM	Physical exfoliation	Water	Freezing the water dispersion at -20 °C for 24 h and then thawing them at 20 °C for 24 h., repeat twice, and sonicated for 4 min with an ultrasonic.	—	4,5
OMTM	Melt exfoliation	Azodicarboxamide (ADC)	Mixing ADC and OMTM at room temperature for 48 h，washing, extruded with polypropylene or polystyrene on a twin-screw extruder at 180 °C, repeat two more times, heated at 210 °C for 10 min.	4	6
OMTM	In-situ exfoliation	E-caprolactam	Mixing 12-aminolauric acid and MTM for 10 min to obtain OMTM, and then heating e-caprolactam and OMTM to 250-270 °C for 48 h to polymerize e-caprolactam.	6.8	7,8
OMTM	Aggregated exfoliation	5-armed starlike polystyrene (PS5)	Synthesis of pentafunctional initiator at 80 °C for 18 h, PS5 syntheses at 90 °C for 24 h, and then mixing the PS5 and OMTM with briefly hand mixed and held unstirred at 220 °C for less than 2 h.	10~15	9
Na-MTM	Aggregated exfoliation	Amine-terminating mannich oligomers (AMO)	Preparation of AMO at 130-170 °C for 4 h, and then mixing the AMO, hydrochloric acid, and Na-MTM at 80-85 °C for 5 h with mechanical stirring.	18	10,11
OMTM	Aggregated exfoliation	Hydroxyl- or carboxy- terminated polybutadiene (HTPB or CTPB)	Mixing OMTM and HTPB or CTPB at 25 °C for 3 min with glass rod stirring and then static ripening them at 80 °C for more than 4 h.	11~15	12,13
OMTM	Aggregated exfoliation	CTPB	Mixing OMTM and CTPB at 25 °C for 3 min with glass rod stirring and then static ripening them at 25 °C for 2 h.	11	14
OMTM	**Aggregated exfoliation**	**Exolit OP 550**	**Mixing OMTM and Exolit OP 550 at 25 °C for 3 min with glass rod stirring.**	**20**	**This work**
OMTM or Na-MTM	**Aggregated exfoliation**	**Exolit OP 550**	**Mixing OMTM and Exolit OP 550 at 25 °C for 3 min with glass rod stirring and then static ripening them at 60 °C for 12 h.**	**30**	**This work**
OMTM	**Aggregated exfoliation**	**Exolit OP 550**	**Mixing OMTM, Exolit OP 550, and ethanol at 25 °C for 3 min with glass rod stirring and then static ripening them at 60 °C for 12 h.**	**100**	**This work**

References

1. H. Ding, Y. Wang, Y. Liang and F. Qin, *Adv. Mater. Sci. Eng.* , 2014, **2014**, 1-8.
2. X.-F. Pan, H.-L. Gao, Y. Lu, C.-Y. Wu, Y.-D. Wu, X.-Y. Wang, Z.-Q. Pan, L. Dong, Y.-H. Song and H.-P. Cong, *Nat. Commun.* , 2018, **9**, 1-8.
3. F. Ding, J. Liu, S. Zeng, Y. Xia, K. M. Wells, M.-P. Nieh and L. Sun, *Sci. Adv.* , 2017, **3**, e1701212.
4. L. Chen, Y. Zhao, T. Chen, H. Bai, T. Zhang, H. Li, Q. An and S. Song, *Results Phys.* , 2019, **15**, 102526.
5. T. Chen, Y. Yuan, Y. Zhao, F. Rao and S. Song, *Langmuir*, 2019, **35**, 2368-2374.
6. O. M. Istrate and B. Chen, *Polym. Int.* , 2014, **63**, 2008-2016.
7. Y. Fukushima and S. Inagaki, in *Inclusion Phenomena in Inorganic, Organic, and Organometallic Hosts*, Springer, 1987, pp. 365-374.
8. A. Usuki, Y. Kojima, M. Kawasumi, A. Okada, Y. Fukushima, T. Kurauchi and O. Kamigaito, *J. Mater. Res.* , 1993, **8**, 1179-1184.
9. D. R. Robello, N. Yamaguchi, T. Blanton and C. Barnes, *J. Am. Chem. Soc.* , 2004, **126**, 8118-8119.
10. C.-C. Chu, M.-L. Chiang, C.-M. Tsai and J.-J. Lin, *Macromolecules*, 2005, **38**, 6240-6243.
11. C.-C. Chou and J.-J. Lin, *Macromolecules*, 2005, **38**, 230-233.
12. X. Wang, F. Tao, G. Xue, J. Zhu, T. Chen, P. Sun, H. H. Winter and A. C. Shi, *Macromol. Mater. Eng.* , 2009, **294**, 190-195.
13. Y. Gao, R. Zhang, W. Lv, Q. Liu, X. Wang, P. Sun, H. H. Winter and G. Xue, *J. Phys. Chem. C*, 2014, **118**, 5606-5614.
14. J. Zhu, X. Wang, F. Tao, G. Xue, T. Chen, P. Sun, Q. Jin and D. Ding, *Polymer*, 2007, **48**, 7590-7597.